

U.S. DEPARTMENT OF COMMERCE  
National Technical Information Service

AD-A033 873

GENERATION OF FRACTION OF A TERAWATT PROTON  
PULSES WITH COAXIAL REFLEX TRIODES

NAVAL RESEARCH LABORATORY, WASHINGTON, D.C.

DECEMBER 1976

005086

NRL Memorandum Report 3422

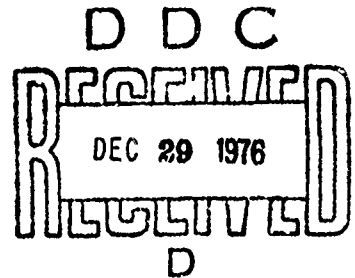
ADA 033873

# Generation of Fraction of a Terawatt Proton Pulses with Coaxial Reflex Triodes

J. GOLDEN, C. A. KAPETANAKOS, S. J. MARSH, AND S. J. STEPHANAKIS

*Experimental Plasma Physics Branch  
Plasma Physics Division*

December 1976



**NAVAL RESEARCH LABORATORY**  
Washington, D.C.

Approved for public release: distribution unlimited.

REPRODUCED BY  
**NATIONAL TECHNICAL  
INFORMATION SERVICE**  
U S DEPARTMENT OF COMMERCE  
SPRINGFIELD VA. 22161

SECURITY CLASSIFICATION OF THIS PAGE (When Data Entered)

REPORT DOCUMENTATION PAGE		READ INSTRUCTIONS BEFORE COMPLETING FORM
1. REPORT NUMBER NRL Memorandum Report 3422	2. GOVT ACCESSION NO.	3. RECIPIENT'S CATALOG NUMBER
4. TITLE (and Subtitle) GENERATION OF FRACTION OF A TERAWATT PROTON PULSES WITH COAXIAL REFLEX TRIODES		5. TYPE OF REPORT & PERIOD COVERED Interim report on a continuing NRL problem.
		6. PERFORMING ORG. REPORT NUMBER
7. AUTHOR(s) J. Golden, C.A. Kapetanakos, S.J. Marsh* and S.J. Stephanakis		8. CONTRACT OR GRANT NUMBER(s)
9. PERFORMING ORGANIZATION NAME AND ADDRESS Naval Research Laboratory Washington, D.C. 20375		10. PROGRAM ELEMENT, PROJECT, TASK AREA & WORK UNIT NUMBERS NRL Problem H02 28A
11. CONTROLLING OFFICE NAME AND ADDRESS Office of Naval Research Arlington, Virginia 22217		12. REPORT DATE December 1976
		13. NUMBER OF PAGES 21
14. MONITORING AGENCY NAME & ADDRESS (if different from Controlling Office)		15. SECURITY CLASS. (of this report) UNCLASSIFIED
		15a. DECLASSIFICATION/DOWNGRADING SCHEDULE
16. DISTRIBUTION STATEMENT (of this Report) Approved for public release; distribution unlimited.		
17. DISTRIBUTION STATEMENT (of the abstract entered in Block 20, if different from Report)		
18. SUPPLEMENTARY NOTES *NRC Research Associate at NRL:		
19. KEY WORDS (Continue on reverse side if necessary and identify by block number) Intense ion beams Ion rings Coaxial reflex triodes		
20. ABSTRACT (Continue on reverse side if necessary and identify by block number) Results are reported on the generation of MeV, pulsed ion beams at a peak power level in excess of $2 \times 10^{11}$ watts that have an angular divergence of about $3^\circ$ - $4^\circ$ . Such beams can be used in the formation of field reversing proton rings.		

DD FORM 1473 JAN 73

EDITION OF 1 NOV 65 IS OBSOLETE  
S/N 0102-014-6601

SECURITY CLASSIFICATION OF THIS PAGE (When Data Entered)

## GENERATION OF FRACTION OF A TERAWATT PROTON PULSES WITH COAXIAL REFLEX TRIODES

### INTRODUCTION

Presently there are several schemes<sup>1-8</sup> available to produce intense, pulsed ion beams. An important motive for the generation of such beams is their potential application to the formation of field reversing ion layers and rings.<sup>9-11</sup> The results of the present experiment demonstrate unequivocally that existing pulsed power technology can provide sufficient ions, in a single pulse, which, if converted into a ring or layer could produce field reversal.

Briefly, in this experiment we have produced hollow, pulsed proton beams in the energy range between 0.6 - 1.2 MeV and peak proton current in excess of 200 kA using a low inductance, coaxial reflex triode (CRT). For the best quality beam produced the angular divergency is between  $3^{\circ}$ - $4^{\circ}$ .

A schematic of the experiment is shown in Fig. 1. The 0.6 to 1.2 MV positive pulse from the GAMBLE II Generator is applied to the anode, which is constructed from solid 12.5  $\mu$ m thick polyethylene film mounted between two 2.3 mm thick concentric stainless steel rings. The outer ring is supported from the inner ring by six 0.65 cm thick radial spokes and the opening between the two rings is about 3 cm, i.e., slightly larger than the thickness of the cathode. To improve the uniformity of the electric field in the anode-cathode gap, the 1.9 cm wide, 14.6 cm inner radius carbon cathode is embedded in the center of a stainless steel half-ring. The surface of the carbon cathode is flush with that of the stainless steel.

Note: Manuscript submitted November 16, 1976.

ACCESSION for	
NTIS	White Section <input checked="" type="checkbox"/>
DDC	Buff Section <input type="checkbox"/>
UNANNOUNCED	
JUSTIFICATION	
BY	
DISTRIBUTION/AVAILABILITY CODES	
Dist.	AVAIL. and/or SPECIAL
A	

In our earlier designs the cathode was a 25 cm I.D., 1.3 cm thick bare carbon ring and the anode was constructed from 12.5  $\mu\text{m}$  thick solid polyethylene film interwoven between 16, 2.5 mm diameter radial spokes. Although this cathode-anode assembly produced very intense beams, their angular divergence was substantially greater than that of beams generated with the embedded cathode.

The protons are extracted out of the plasma formed from the plastic by the oscillating electrons. The ions that are accelerated toward the virtual cathode, by the positive potential on the anode, pass through it and form a drifting beam.

To maximize the energy delivered to the electrons and ions, i.e., the resistive part of the load in the reflex triode, it is necessary that the inductance of the triode be kept as small as possible. This has been accomplished by designing the triode in such a way that the current flows in a coaxial configuration. For the 20 cm long anode stalk (inner conductor) of 9.5 cm radius and the 12.7 cm radius outer conductor the inductance of the load is about 12 nH. The electrical breakdown in the vacuum gap between the inner and outer conductors is prevented by the externally applied axial magnetic field. The critical<sup>12</sup> magnetic field  $B_c$  required to magnetically insulate the 3.2 cm gap between the two coaxial cylinders is less than 1.5 kG.

The total number of protons in the beam is measured by a nuclear activation technique (NAT)<sup>2-6,13</sup>. This technique not only gives information about the total number of protons in the pulse  $N_p$ , but also allows an unambiguous identification of protons. Briefly, the activation technique employed in the present experiment consists of measuring the

radioactivity induced on a carbon target by the beam. The number of protons is inferred from the measured number of delayed  $\gamma$ -rays associated with the annihilation of positrons ( $\beta^+$ ), that are produced from the resonant reaction  $^{12}\text{C}(p,\gamma)^{13}\text{N}(\beta^+)^{13}\text{C}$ . In the coincidence counting the only  $\gamma$ -rays recorded are those with energy between 0.45 - 0.55 MeV. At the higher energies the number of counts is corrected for the  $^{12}\text{C}(d,n)^{13}\text{N}(\beta^+)^{13}\text{C}$  reaction induced by the natural isotopic abundance of deuterium in polyethylene. The number of counts is not corrected for target "blow-off", i.e., the loss of the radioactive  $^{13}\text{N}$  nuclei prior to detection. When the target is situated several cm from the anode, the "blow-off" correction appears to be small. This was determined by comparing the radioactivity induced in a target by a portion of the full intensity beam with the radioactivity induced in another target by a portion of the beam that was attenuated by passage through metal screens of known transmission. The total number of protons measured with the NAT ( $N_p \approx 4 \times 10^{16}$ /pulse with the bare carbon cathode;  $N_p > 3 \times 10^{16}$ /pulse with the embedded cathode) is less than a factor of two smaller than that determined from calorimetry measurements. Peak ion currents in excess of 200 kA, at 1 MeV are inferred from the number of protons measured by the NAT and the ion pulse shape determined approximately with a scintillator-photodiode system. Near the anode, this peak current corresponds to a peak ion current density of about 1 A/cm<sup>2</sup>. At  $V = 1$  MV and an anode-cathode spacing of 2 cm the predicted bipolar ion current density is about 36 A/cm<sup>2</sup>, i.e., appreciably smaller than that observed. To verify that protons are

accelerated not only toward the virtual cathode but also toward the real cathode, the radioactivity induced on a segment of the carbon cathode was measured after a shot. The results show that, as expected, the number of protons propagating in one direction (virtual cathode) is comparable to those propagating toward the other (real cathode). Attempts to measure the ion current with biased ion collectors (BIC) or Faraday cups have been unsuccessful. Consistent with our previous experience<sup>2-6</sup>, we have found that both the shape and the magnitude of their output are unreliable.

Waveforms from a typical shot are shown in Fig. 2. The output of the scintillator-photodiode detector first appears about 45 nsec after the beginning of the corrected voltage. This delay is consistent with the time required by the ions of energy about equal to the triode voltage to travel the anode-scintillator distance. An interesting feature of the results is the slow rise of the total current. The total current flowing in the device is monitored in three different positions using two pick-up loops and a shunt resistor. In general the three monitors agree and we can account for the occasional difference in their shape occurring for very long times (usually 80-100 nsec after the initiation of the voltage pulse). At early time, the output of the shunt resistor shows a step like behavior. This jump is associated with the time derivative of the applied voltage ( $dV/dt$ ) and is absent for small  $dV/dt$ . This has been determined by varying  $dV/dt$  that is accomplished by changing the opening of the prepulse switch.

The rise time of the current waveforms is comparable to the dura-

tion of the voltage pulse and cannot be attributed to inductive effects, because for an appreciable fraction of the voltage pulse duration the time  $L/(R_{\text{gen}} + R_{\text{triode}})$  is less than 10 - 15 nsec, i.e., several times shorter than the pulse duration.

The slow rise of the current cannot also be explained by the progressive closing of the anode-cathode gap as a result of the anode-cathode plasma expansion. For a 12.5  $\mu\text{m}$  thick polyethylene anode film the energy flux required to ionize the  $3.4 \times 10^{19}/\text{cm}^2$  hydrogen and  $1.7 \times 10^{19}/\text{cm}^2$  carbon atoms and raise the temperature of the plasma to 1 eV is about 116 Joule/ $\text{cm}^2$ , i.e., greater than the available energy for most of our shots. (It should be noted that even at a plasma temperature of 1 eV, the Saha equation predicts an almost fully ionized plasma).

Although there is presently insufficient evidence to draw a definite conclusion, it is possible that the observed effect is associated with the absence of a steady state in the triode when the magnitude of the ion current  $I_i$  flowing in the device approaches that of the electron current  $I_e$ . This explanation is consistent with the observation that the total current shows a very fast rise at early times and remains practically flat for almost the entire duration of the voltage pulse when  $I_e \gg I_i$ . Figure 3 shows the voltage and the output of the shunt resistor when  $I_e \gg I_i$ . This has been accomplished by limiting the amount of anode plasma and thus the number of ions available for extraction. The amount of anode plasma is limited by reducing the flash-over plasma production by means of a 6  $\mu\text{m}$  thick aluminized mylar film

attached to the regular 12.5  $\mu\text{m}$  thick polyethylene anode.

In addition, the explanation is consistent with the predictions of some recent computer simulation experiments<sup>14</sup>.

Within the anode-cathode gap the self magnetic field  $B_\theta$  varies as  $1/r$  between the anode stalk and the inner edge of the hollow beam and decreases to zero at the outer edge of the beam. Typically the magnitude of  $B_\theta$  is several kG and has a pronounced effect on the orbits of the oscillating electrons. The effect of  $B_\theta$  is diminished when it becomes smaller than the externally applied field  $B_z$ . Figure 4 shows the voltage, current, impedance and x-ray waveforms for four different values of  $B_z$ . For  $B_z = 0$ , a large fraction of the electrons strikes the outer ring of the anode as a result of the outward radial drift  $v_r = E_z/B_\theta$  acquired by these electrons during their first crossing of the cathode-anode gap. The observed current is limited to the critical current<sup>15</sup> resulting in a very high triode impedance and low ion current.

The outward radial motion of electrons is restricted by the application of an axial magnetic field. For  $B_z \gtrsim B_\theta$ , the electron motion becomes approximately one dimensional and the electron life time, i.e., the number of transits through the anode plastic, is substantially greater than when  $B_\theta \gg B_z$ . The result is a high ion current and a low triode impedance.

The above qualitative remarks about the electron orbits have been verified by a relativistic but non-self-consistent computer calculation. Results are shown in Fig. 5. In addition, the reduction of the x-ray signal with increasing  $B_z$  is in agreement with the above interpretation.

of the results. The lower x-ray output cannot be explained by the reduction in the applied voltage since the quantity  $v^2 \cdot B_z$  decreases by less than a factor of 2.5 as  $B_z$  varies from 0 to 7.7 kG while the x-ray signal varies considerably more than an order of magnitude.

High trapping efficiency of a rotating ion beam in a magnetic mirror field requires the angular divergence of such a beam to be small. Among the various anode-cathode assemblies tested the embedded cathode appears to produce the best quality beams. The angular divergence is determined by measuring the thickness of the beam by streak photography (streaking speed of 0.25 mm/nsec). A streak photograph of a 0.8 cm wide strip of aluminized scintillator aligned along a diameter from a radius of 4.75 cm to 18.75 cm and located at 0.5 m from the anode is shown in Fig. 6. The scintillator strip is tilted  $\sim 30^\circ$  with respect to the vertical axis. The narrow, prompt signal appearing at an approximately 17 cm radius is probably due to electrons. The wide part of the image corresponding to the proton pulse has approximately the same duration as the high voltage pulse. It can be shown that for  $t > \pi/\omega_{ci}$  the angular divergence  $\theta$  is related to the beam thickness  $d$  by the relation

$$\sin\theta = \omega_{ci} (d - \Delta\rho) / 2v_0, \quad (1)$$

where  $\omega_{ci}$  is the ion cyclotron frequency at the measuring position,  $\Delta\rho$  is the thickness of the beam at the anode and  $v_0$  is the speed of the ions. For the best quality beams the above relation gives  $\theta \approx 3^\circ - 4^\circ$ . The radial profile of the beam is determined by individually counting

small segments of a carbon target after being activated by the proton beam. Profiles for the bare carbon (a) and for the improved design with an embedded cathode (b) are shown in Fig. 7. The approximate width at half maximum of the radial profiles shown are 13 cm (Fig. 7a) and 8 cm (Fig. 7b) corresponding to a mean angular divergence of approximately  $10^\circ \pm 4.5^\circ$  and  $5.5^\circ \pm 3.3^\circ$  respectively. This is in agreement with the streak photography which gives about  $3^\circ - 4^\circ$  with the embedded cathode.

The present results clearly demonstrate that low impedance coaxial reflex triodes can efficiently produce MeV proton beams at a fraction of a terawatt power level. The generation of low divergence, high power beams is an essential step toward the realization of field reversing ion layers and rings.

## ACKNOWLEDGMENTS

We are grateful for the help given us by Dr. R.A. Mahaffey. Also discussions with Drs. A.E. Robson, Shyke Goldstein, A.T. Drobot, and Roswell Lee have been very helpful. The technical assistance of R.A. Covington, R.M. Lowery, J.W. Snider, and E.A. Bellifiore is greatly appreciated.

#### REFERENCES

1. S. Humphries, T.J. Lee and R.N. Sudan, Appl. Phys. Lett. 25, 20 (1974); also J. Appl. Phys. 4, 187 (1975). S. Humphries, R.N. Sudan and L. Willey, J. Appl. Phys. 37, 2382 (1976).
2. C.A. Kapetanacos, J. Golden and F.C. Young, Nuclear Fusion 16, 151 (1976).
3. J. Golden and C.A. Kapetanacos, Appl. Phys. Lett. 28, 3 (1976).
4. J. Golden, C.A. Kapetanacos and S.A. Goldstein, Proc. of the 7th European Conf. on Cont. Fusion and Plasma Physics, Lausanne, 1-5 September 1975, Vol. 1, p. 91.
5. J. Golden, C.A. Kapetanacos, R. Lee and S.A. Goldstein, Proc. of Intl. Top. Conf. on Electron Beam Research and Technology, Albuquerque, N.M., Nov. 3-5, 1975, Vol. 1, p. 635.
6. C.A. Kapetanacos, J. Golden and W.M. Black, Phys. Rev. Lett. 37, 1236 (1976).
7. S.J. Stephanakis, D. Masher, G. Cooperstein, J.R. Boller, J. Golden and S.A. Goldstein, sub. to Phys. Rev. Lett.
8. D.S. Prono, J.W. Shearer and R.J. Briggs, Phys. Rev. Lett. 37, 21 (1976).
9. H.H. Fleischmann, in Electrostatic and Electromagnetic Confinement of Plasma (Proc. Conf. New York, 1974) N.Y. Academy of Sciences (1974).
10. R.N. Sudan and E. Ott, Phys. Rev. Lett. 33, 355 (1974).

11. C.A. Kapetanakos, R.A. Parker and K.R. Chu, Appl. Phys. Lett. 26, 284 (1975).
12. T.J. Orzechowski and G. Bekefi, Phys. Fluids 19, 43 (1976).
13. F.C. Young, J. Golden and C.A. Kapetanakos, Diagnostics for Intense Pulsed Ion Beams, NkL Report No. 3391 (1976).
14. R. Lee, C.A. Kapetanakos, J. Golden and S.A. Goldstein, Bull. Amer. Phys. Soc. 21, 691 (1976).
15. S.A. Goldstein, R.C. Davidson, J.G. Siambis, and R. Lee, Phys. Rev. Lett. 33, 1471 (1974).

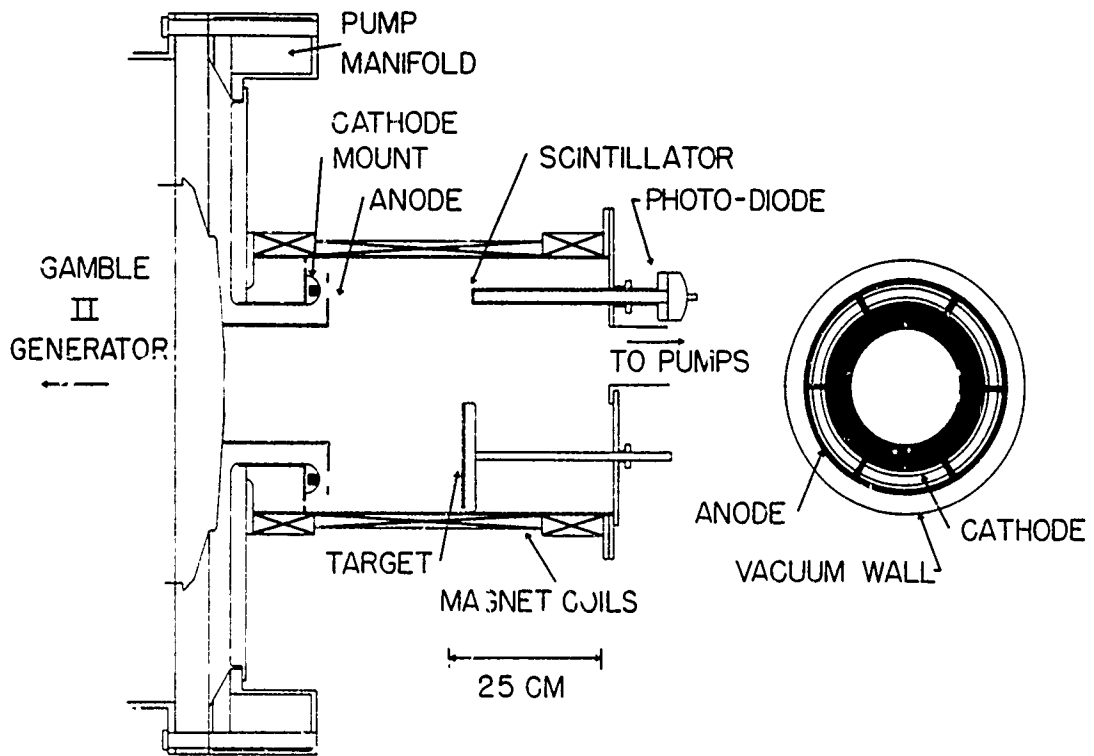


Fig. 1 — Schematic of the experiment

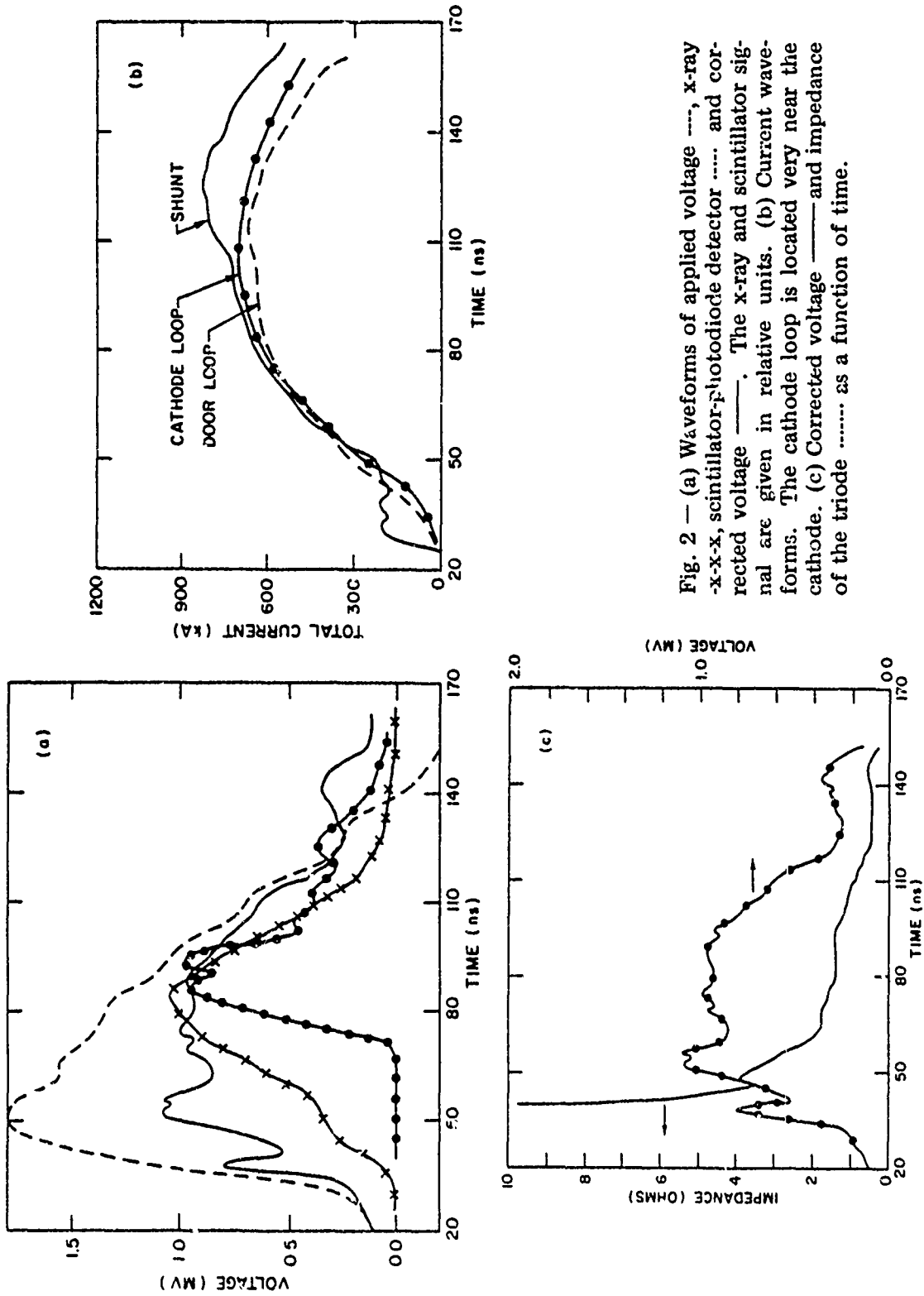


Fig. 2 — (a) Waveforms of applied voltage ----, x-ray -x-x-x, scintillator-photodiode detector ..... and corrected voltage ——. The x-ray and scintillator signal are given in relative units. (b) Current waveforms. The cathode loop is located very near the cathode. (c) Corrected voltage ——— and impedance of the triode ..... as a function of time.

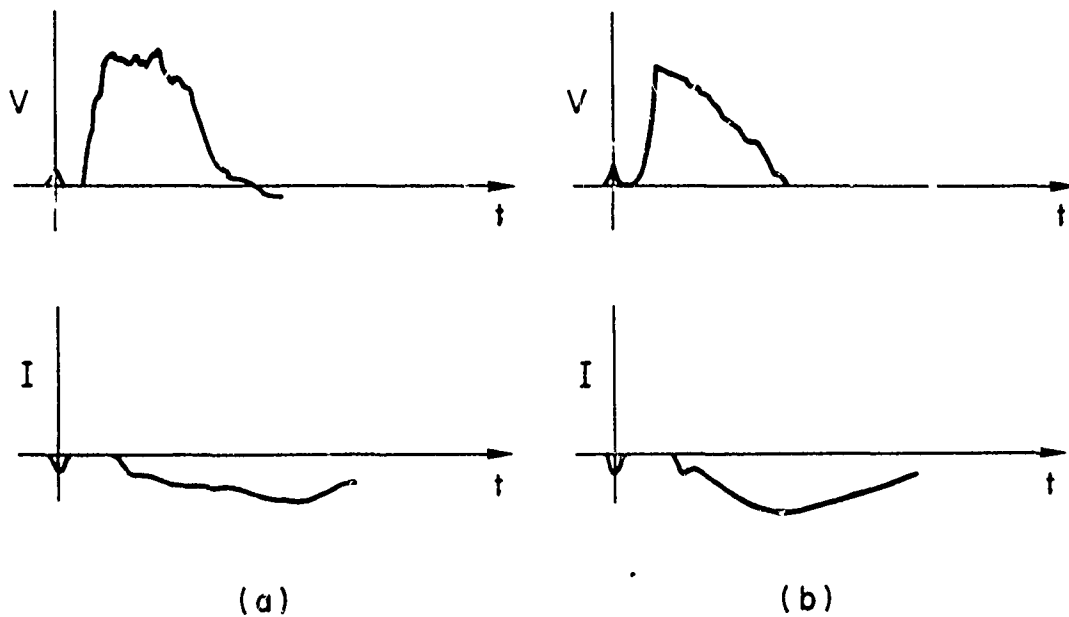


Fig. 3 — Oscilloscope traces of applied voltage and current (shunt) for a  $6\ \mu\text{m}$  thick aluminized mylar attached to  $12.5\ \mu\text{m}$  thick polyethylene anode (a) and a  $12.5\ \mu\text{m}$  thick polyethylene anode (b)

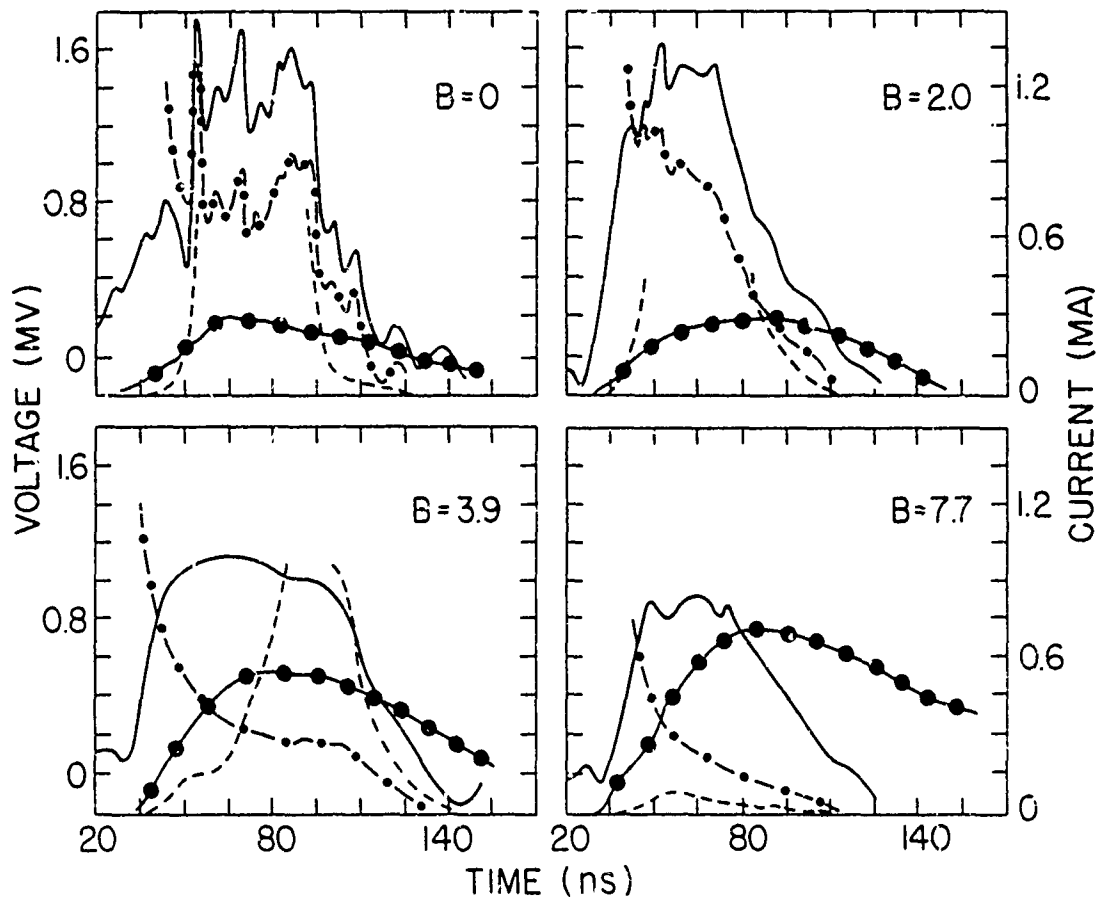


Fig. 4 — Typical waveforms at various applied magnetic fields. Shown are the corrected voltage (solid line), anode current (large dots), x-ray signal (dashed line), and impedance (dot-dashed line). The x-rays are given in relative units, and the impedance is 1 Ohm/div (right vertical axis).

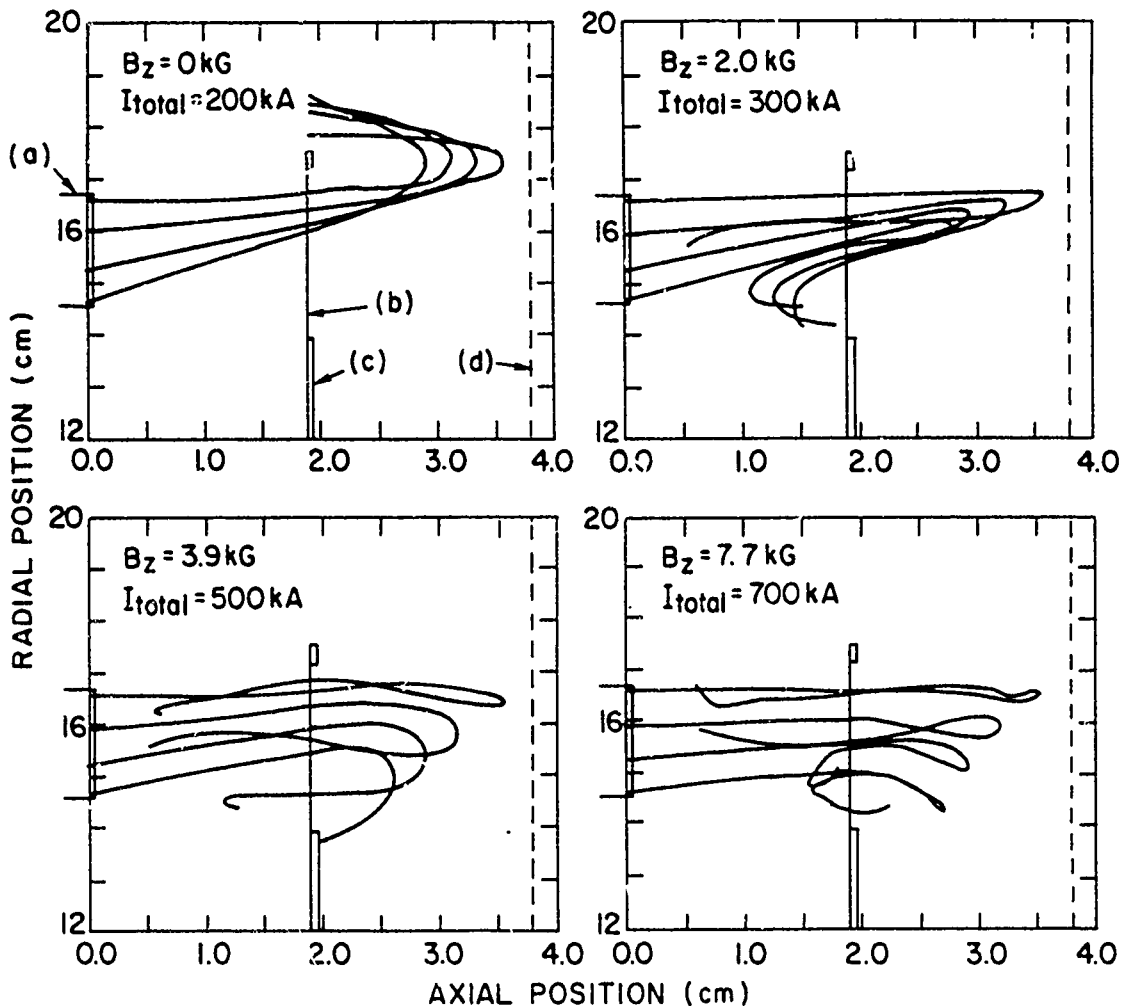


Fig. 5 — Computed orbits of electrons inside the triode for four different values of externally applied magnetic field  $B_z$  and the total current. Shown are the cathode (a), plastic anode film (b), stainless steel anode support (c) and assumed position of the virtual cathode. The axial electric field is taken equal to zero at both the cathode and anode surfaces.

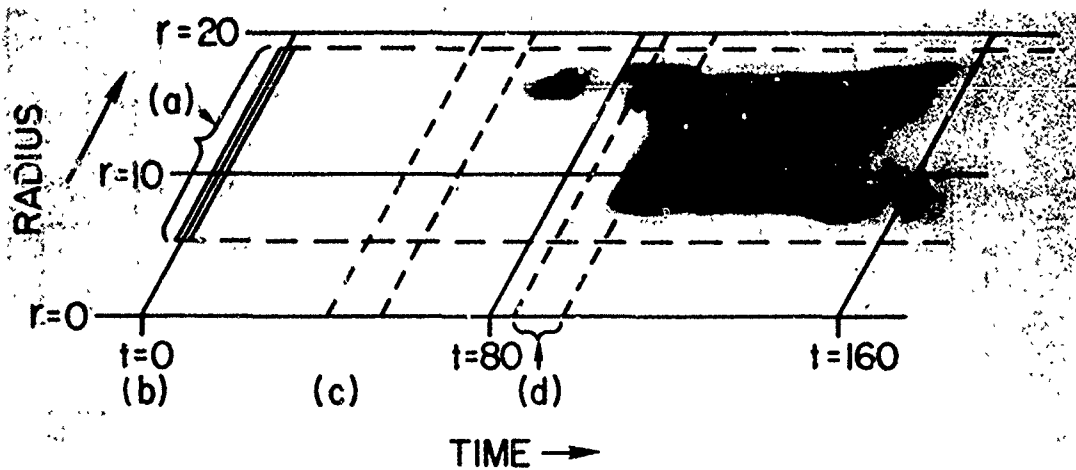


Fig. 6 — Streak photograph of the ion beam. Shown are (a) the initial image of the scintillator strip, (b) the beginning of the streak (c) the beginning of the high-voltage pulse, and (d) the expected time of arrival for the protons.  $B_z = 2$  kG at the scintillator.

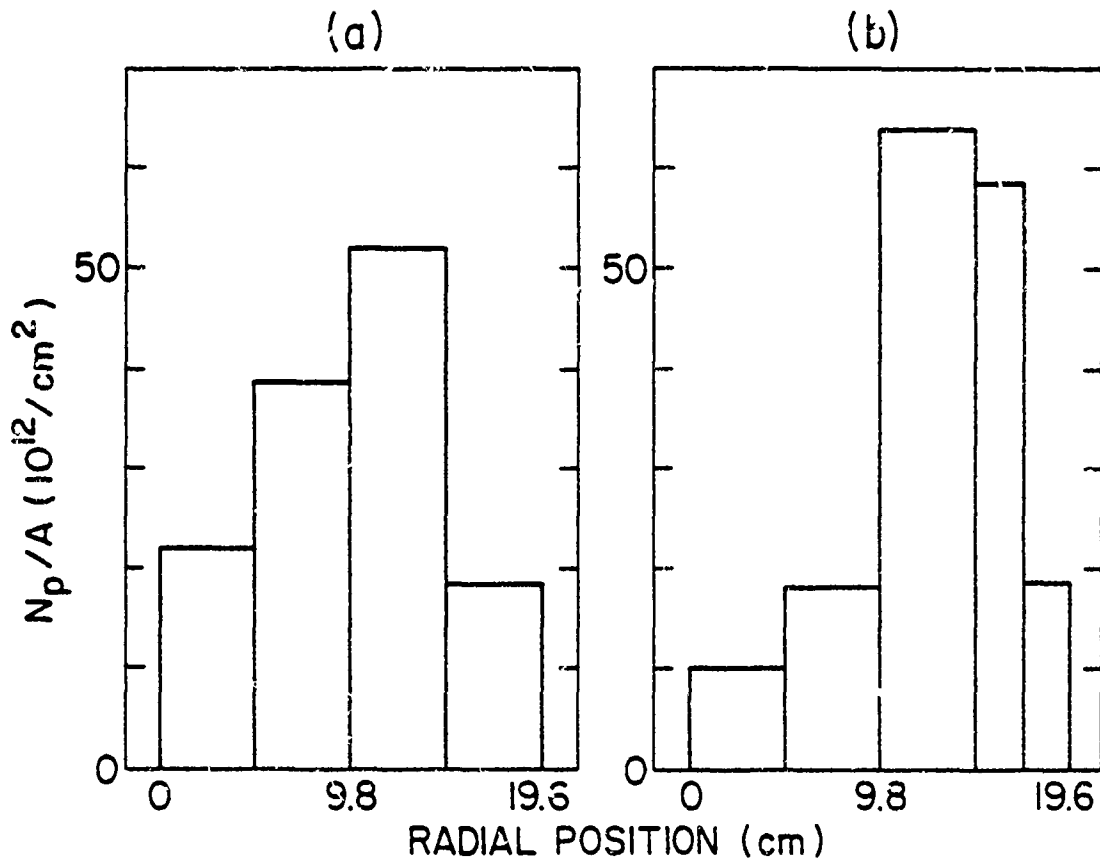


Fig. 7 — The radial beam profile at 25 cm from the anode for a peak applied magnetic field of 3.9 kG (a) bare cathode and (b) embedded cathode